

RSC Advances



This is an *Accepted Manuscript*, which has been through the Royal Society of Chemistry peer review process and has been accepted for publication.

Accepted Manuscripts are published online shortly after acceptance, before technical editing, formatting and proof reading. Using this free service, authors can make their results available to the community, in citable form, before we publish the edited article. This *Accepted Manuscript* will be replaced by the edited, formatted and paginated article as soon as this is available.

You can find more information about *Accepted Manuscripts* in the [Information for Authors](#).

Please note that technical editing may introduce minor changes to the text and/or graphics, which may alter content. The journal's standard [Terms & Conditions](#) and the [Ethical guidelines](#) still apply. In no event shall the Royal Society of Chemistry be held responsible for any errors or omissions in this *Accepted Manuscript* or any consequences arising from the use of any information it contains.

Electrochemical Behavior of Sn-Graphene Composite Coating

Rohit Berlia, Punith Kumar M.K., and Chandan Srivastava*

Dept. of Materials Engineering, Indian Institute of Science (IISc), Bangalore- 560012

*Corresponding author. Tel: +91-80-22932834

E-mail address: csrivastava@materials.iisc.ernet.in (Chandan Srivastava)

Abstract

Electrochemical properties of pure Sn and Sn-graphene composite coating have been determined and compared. Coatings were electrodeposited on mild steel substrates. Graphene was synthesized by the electrochemical exfoliation process using SO_4^{2-} ion as the intercalating agent. Morphological and structural characterization results revealed a clear effect of graphene on altering the texture, grain size and morphology of the coating. Corrosion behavior was analyzed through potentiodynamic polarization and electrochemical impedance spectroscopic methods. A significant improvement in the corrosion resistance in terms of reduction in corrosion current and corrosion rate and increase in polarization resistance was noted in case of Sn coating containing graphene.

Keywords: Sn–graphene composite coating, Electrodeposition, Corrosion.

1. Introduction

Graphene has attracted considerable attention due to its remarkable optical,¹ mechanical,² thermal³ and electronic properties⁴. Recently, it has been demonstrated that impermeable and chemically stable coating of multilayer graphene on metallic substrates protects the substrates against degradation in highly corrosive environments.^{5,6} With respect to the traditional metallic coatings that are used for corrosion protection,^{7,8} it has been demonstrated that addition of graphene into the metallic coatings results in a considerable enhancement in the anti-corrosive behaviour^{9,10}. It has been shown that the corrosion resistance of Ni-graphene⁹ and Zn-graphene¹⁰ composite coatings is considerably higher than the corrosion resistance of pure Ni and Zn coatings. Enhancement in the anti-corrosive property has been attributed primarily to the effect of graphene in impeding the formation of pits in the coatings and alterations in the morphology and texture of the coatings.^{9,10}

One of the widely used pure metal coating for corrosion protection is Sn coating. Use of Sn for plating purposes dates back to 19th century. Currently, Sn is extensively used in coating beverage cans and in food packaging.¹¹ Although, several studies have been done on the electrodeposition and corrosion behavior of Sn coatings, focus on methodologies that can be adopted to enhance the anti-corrosive properties of Sn coating is missing. Furthermore, there is no report yet on the investigation of texture, morphology and electrochemical properties of Sn-graphene composite coating. This work focuses on the generation of Sn-graphene composite coating over mild steel substrate using acidic Sn chloride bath containing graphene produced by the electrochemical exfoliation method. As-fabricated Sn and Sn-graphene composite coatings

were characterized and subjected to electrochemical analysis to evaluate and compare their corrosion behavior.

2 Experimental

Chemicals were purchased from SD fine chemicals India Ltd. and chemicals were used in the form of as supplied. Graphene was synthesized by the electrochemical exfoliation process using two graphite electrodes. One of them was used as cathode and other as anode. Platinum foil was used as the reference electrode. The exfoliation process was carried out in 0.05M sodium sulphate solution at 5V for 10 hours using simple DC source. The exfoliated graphene was isolated by centrifuging at 10000 rpm for 10 min and further ultrasonicated to separate thin graphene layers. Na_2SO_4 is a water soluble compound, hence the graphene sample was centrifuged and the supernatant liquid containing dissolved sodium sulphate was decanted. Again fresh water was added to the conical tube containing settled graphene, sonicated and centrifuged and the dissolved sodium sulphate was removed by decanting the supernatant liquid. Same procedure was followed for several times to remove the dissolved sodium sulphate.

Tin was electrodeposited on mild steel substrate using a two electrode system and a simple DC source. Mild steel substrate acted as cathode while platinum foil acted as counter electrode. Before electrodeposition, the steel substrate was finely polished, degreased using acetone and activated by dipping in 10 % HCl solution. Electrolyte was prepared by dissolving 9.2 gm L^{-1} of SnCl_2 , 26.7 gm L^{-1} of NH_4Cl , 30.9 gm L^{-1} of H_3BO_3 and 43.6 gm L^{-1} of sodium gluconate in distilled water. Current density of 6.5 mA cm^{-2} was applied for 20 min to uniformly coat the mild steel substrate. pH of solution was maintained at 3.5. Deposition was carried out at room temperature under continuous stirring at 100 rpm. The Sn+G (tin + graphene) composite

coating was prepared from the Sn plating bath into which 50 mg L^{-1} of graphene was dispersed. All other deposition parameters were kept constant. Graphene present in the electrolyte was uniformly dispersed by continuously stirring at 350 rpm and sonicating for 12 hrs.

Surface morphology of the samples was analyzed by using JEOL-JEM-1200-EX II scanning electron microscope (SEM) operating at 25kV. SEM was fitted with an energy dispersive spectroscopy (EDS) detector from compositional analysis. X-ray diffraction (XRD) profiles were obtained using the X-pert Pro X-ray diffractometer employing a $\text{Cu } k_{\alpha}$ ($\lambda=0.15400\text{nm}$) radiation source. UV-Visible absorption spectroscopic experiments were carried in 700 to 200 nm wavelength range using Perkin Elmer (Lambda 35) UV-Vis Spectrometer. Raman spectrum of the graphite, graphene and Sn-G composite coating samples were obtained using microscope setup (HORIBA JOBIN YVON, Lab RAM HR) consisting of Diode-pumped solid-state laser operating at 532 nm with a charge coupled detector. Electrochemical corrosion analysis of Sn and Sn-graphene coatings were performed using three electrode system in CH604E electrochemical workstation. 3.5 wt% NaCl solution was used as the electroactive media. 1cm^2 area of the coating exposed to the electroactive media acted as the working electrode. Reference electrode used for the corrosion measurement was Ag/AgCl. Platinum foil acted as the counter electrode. Electrochemical impedance data was curve fitted using ZSimp Win 3.21 software.

3. Results and Discussion

Graphene used for Sn+G composite coating was prepared by electrochemical exfoliation of graphite in Na_2SO_4 electroactive media. Sulphate ion based compounds are generally used to exfoliate graphite^{12,13} because of the fact that the SO_4^{2-} ion size (0.46 nm) is larger than the

interlayer spacing (0.335 nm) between the graphitic layers.^{16,17} Large size of the sulphate ion destabilizes and weakens the attractive force between the graphite layers during the intercalation facilitating the production of graphene. XRD profile and UV-Visible absorption spectrum obtained from the exfoliated graphene sample is shown respectively in Fig. 1(a) and 1(b). The characteristic broad peak at $25^\circ 2\theta$ value in the XRD profile and the maximum optical absorption (λ_{\max}) around 270 nm in UV-Visible absorption spectrum confirmed the presence of graphene in exfoliated product.¹³⁻¹⁵ The broad XRD peak observed for the graphene samples illustrates disordering of the initial graphitic structure and decrease in number of stacked graphene layers in the exfoliated product.¹³ Furthermore, absence of graphene oxide characteristic diffraction peak at $14^\circ 2\theta$ in the XRD profile and absorption peak (λ_{\max}) around 230nm in UV-Vis spectrum confirmed that the exfoliated samples did not contain graphene oxide.^{13,16}

Three major peaks in the Raman spectra obtained from the graphite, graphene and Sn+G composite coatings are shown in Fig. 2. The D band at $\sim 1361\text{ cm}^{-1}$ corresponds to the presence of SP^3 defects, G band around $\sim 1580\text{ cm}^{-1}$ corresponds to the phonon mode in-plane vibration of SP^2 carbon atoms and 2D band at $\sim 2700\text{ cm}^{-1}$ corresponds to two phonon lattice vibration.¹⁷ However, the appearance of D, G and 2D band in the Raman spectra of Sn-G composite coating is confirmed the incorporation of graphene layers in Sn metal matrix. The defect density of the graphitic structures was determined by measuring the I_D/I_G ratio (I_D and I_G -intensity of D and G band).¹⁸ The defect density corresponding to graphite, graphene and the graphene incorporated in Sn metal matrix were 0.977, 1.169 and 0.646 respectively. The calculated I_D/I_G ratio interestingly revealed that the defect density of the graphene layers is considerably reduced after its incorporation in the Sn metal matrix.

SEM-EDS analysis over the cross section of Sn+G composite coating is depicted in Fig. 3. The EDS analysis revealed the presence of approximately 2.54 wt% of carbon in the Sn+G composite coating indicating the incorporation of graphene dispersed in plating bath into the growing Sn metal matrix during the electrodeposition process. The measured thickness of Sn and Sn+G composite coatings through the cross section of the films is around 21 μm . Representative SEM micrographs of Sn and Sn+G composite coatings are provided in Fig. 4. A morphology characterized by randomly oriented cubes can be observed for both the coatings. A degradation of the cube morphology is however clearly evident in case of the graphene containing coating.

XRD profile obtained from both the coatings is provided in Fig. 5. Average crystallite size for Sn and Sn+G coatings calculated by using the Scherrer formula¹⁹ was 79.46 ± 3.8 nm and 75 ± 2.3 nm respectively. Incorporation of graphene into the growing Sn metal matrix decreased the crystallite size. The decrease in grain size is possibly due to two factors; (a) incorporation of graphene into the growing metal matrix provides more surface area for heterogeneous nucleation and (b) graphene increases the deposition potential by blocking the active cathode surface area which leads to finer grain size followed by impeded crystal growth. A similar effect of the second phase particle on grain size refinement due to cathodic polarization, as seen in the present case, has been reported by Chu et al.²⁰ for Sn-SiC composite and by Sajjadnejad et al²¹ for Zn-SiC composite. Texture coefficient values calculated from Eq 1²² for the XRD profiles of Sn and Sn+G coatings are provided in Fig. 6. Comparison of the texture coefficients and the XRD profiles clearly reveals the effect of graphene in altering the texture of the Sn coating. Modification of the cathodic surface energy due to the adsorption of graphene during crystal growth can change texture. A similar alteration in texture due to change in cathodic surface energy in case of Sn coatings containing SiC as the second phase particles has been reported by

Chu et al.²⁰ Crystal growth along (2 0 0), (3 0 1) and (4 0 0) crystallographic plane is considerably enhanced in case of Sn+G composite coating when compared to the crystal growth direction in case of pure Sn coating. These results are in agreement with the literature that an incorporation of second phase materials to a growing metal matrix can affect the grain size and the preferred orientation of the deposit.^{22,23}

$$T_c(\text{hkl}) = \frac{I(\text{hkl})}{\sum I(\text{hkl})} \times \frac{\sum I_o(\text{hkl})}{I_o(\text{hkl})} \quad \text{----- (1)}$$

where, $T_c(\text{hkl})$ is the Texture coefficient; $I(\text{hkl})$ is Peak intensity of the Sn electrodeposits; $\sum I(\text{hkl})$ - Sum of intensities of the independent peaks and the index 'o' refers the intensities for the standard Sn sample.

Electrochemical corrosion analysis was performed for the Sn and Sn+G composite coatings. Tafel curves or potentiodynamic polarization curves provided in Fig. 7 were measured by polarizing the working electrode to ± 200 mV against the open circuit potential at the scan rate of 10 mV S^{-1} . The polarization curve corresponding to the Sn+G composite coating was shifted to less negative potential side compared to the position of the polarization curve corresponding to the pure Sn coating. The corrosion potential (E_{corr}) values for the Sn and Sn+G composite coatings were -0.573 V and -0.537 V respectively. This clearly indicated that the composite coating required more potential to release electron when compared to the potential required to corrode the pure Sn plated surface. Corrosion current (I_{corr}) and corrosion rate (CR) values were obtained from the Tafel polarization curves. The I_{corr} and CR values obtained for the pure Sn coating were $1.365 \pm 0.059 \text{ } \mu\text{A cm}^{-2}$ and $1.480 \pm 0.077 \text{ } \mu\text{g h}^{-1}$ respectively. The I_{corr} and CR values obtained for the Sn+G coating were $0.815 \pm 0.043 \text{ } \mu\text{A cm}^{-2}$ and $0.896 \pm 0.056 \text{ } \mu\text{g h}^{-1}$ respectively.

The corrosion parameter valued revealed that the graphene incorporated Sn coating is more stable towards aggressive media when compared to the pure Sn coating.

The electrochemical impedance spectroscopic (EIS) measurements were carried out at the open circuit potential value of the corresponding working electrode in the frequency range of 1 MHz to 100 mHz at a data density of 6 points per decade frequency with sinusoidal signal amplitude of 5 mV. The obtained EIS data are plotted as Nyquist plot shown in Fig. 8(a). Two capacitive loops observed in Fig. 8(a) clearly indicate that the corrosion process consisted of two relaxations. Also, width of the capacitive loop which is a measure of corrosion resistance or polarization resistance (R_p) was significantly higher for Sn+G composite coating when compared to the loop width for the Sn coating. This clearly indicated better anticorrosive behavior of the Sn+G composite coating. To calculate the corrosion parameters, the EIS data was curve fitted using 2RC electrical equivalent circuit (EEC) with the help of ZSimp win 3.21 software. The corresponding EEC^{24,25} is given in Fig. 8(b). To obtain better results the capacitive elements were replaced with constant phase element (CPE). Contribution of each element in EEC in Fig. 8(b) is as follows:

R_e is the electrolyte resistance between the reference electrode and the surface of the working electrode.

The high frequency contribution ($Q_{coat}-R_{coat}$) is ascribed to the dielectric character (Q_{coat}) of the coating that is reinforced by ionic conduction through its pores (R_{coat}).

The low frequency contribution is attributed to the double layer capacitance (C_{dl}) at the electrolyte/coated surface interface at the bottom of the pores coupled with the charge transfer resistance (R_{ct}).

Total polarization resistance (R_p) is the sum of R_{coat} and R_{ct} (i.e., $R_p = R_{coat} + R_{ct}$) and it corresponds to the extent of anti-corrosive character of the coating. The polarization resistance of Sn and Sn+G coating was found to be 10925 Ω and 47770 Ω respectively. These values clearly revealed that the corrosion resistance or polarization resistance of Sn coating is significantly enhanced due to the incorporation of graphene into the metal matrix. Double layer capacitance value obtained for the Sn and Sn+G coating was 149.2 $\mu\text{F cm}^{-2}$ and 69.68 $\mu\text{F cm}^{-2}$ respectively. Decrease in the double layer capacitance value indicates a decrease in the charge accumulation on the Sn+G composite coating. A decrease in the charge accumulation leads to a decrease in the electrochemical activity and a corresponding enhancement of the anticorrosive property of the Sn+G coating.

The scanning electron micrographs of corroded Sn and Sn+G coating are given in Fig. 9. The absence of considerable pits in the SEM images reveals uniform corrosion of the coatings. However, Fig. 9 clearly shows that the Sn coated surface is more deteriorated compared to Sn+G composite coatings. The present work clearly illustrates that an addition of graphene into Sn metal matrix influences the microstructure of the deposit and makes it considerably more nobler than the pure Sn coating.

4. Conclusion

Pure Sn and Sn+Graphene composite coating were electrodeposited on mild steel substrates. Electrochemical exfoliation of graphite electrode was used to produce graphene. Incorporation of graphene into Sn coating led to changes in morphology, grain size and texture of the deposit. Addition of graphene resulted in a significant increase in polarization resistance and decrease in the corrosion rate. Also, a decrease in double layer capacitance for Sn+G coating

with increased polarization resistance confirmed the better electrochemical anticorrosive behavior of Sn+G composite coating when compared to pure Sn coating.

Acknowledgement

Authors acknowledge research funding from Joint Advanced Technology Program (JATP), Indian Institute of Science, Bangalore, India. C. Srivastava acknowledges the research grant received from DST-Nano Mission grant.

References:

- 1 F. Bonaccorso, Z. Sun, T. Hasan and A. C. Ferrari, *Nature Photonics*, 2010, **4**, 611 – 622.
- 2 I.A. Ovid'ko, *Rev. Adv. Mater. Sci.*, 2013, **34**, 1–11.
- 3 E. Pop, V. Varshney and A. K. Roy, *MRS Bull.*, 2012, **37**, 1273– 1281.
- 4 A. H. Castro Neto, F. Guinea, N. M. R. Peres, K. S. Novoselov and A. K. Geim, *Rev. Mod. Phys.*, 2009, **81**, 109-162.
- 5 D. Prasai, J. C. Tuberquia, R. R. Harl, G. K. Jennings and K. I. Bolotin, *ACS Nano*, 2012, **6(2)**, 1102-1108.
- 6 Y. Su, V. G. Kravets, S.L. Wong, J. Waters, A. K. Geim and R. R. Nair, *Nat. Commun.*, 2014, **5**, 4843(1-4).
- 7 J. Havlik, A. Kalendova and D. Vesely, *J. Phys. Chem. Solids*, 2007, **68**, 1101-1105.
- 8 M. Lekka, D. Koumoulis , N. Kouloumbi and P.L. Bonora, *Electrochim. Acta*, 2009, **54**, 2540-2546
- 9 C. M. Praveen Kumar, T. V. Venkatesha and R. Shabadi, *Mater. Res. Bull.*, 2013, **48(4)**, 1477-1483.
- 10 M. K. Punith Kumar, Mahander Pratap Singh and Chandan Srivastava, *RSC Adv.*, 2015, **5**, 25603-25608.
- 11 Alan M Russell and Kok Loong Lee, “Structure property relations in non-ferrous metals” John Wiley and Sons, New Jersey (2005)
- 12 K. Parvez, R. Li, S. R. Puniredd, Y. Hernandez, F. Hinkel, S. Wang, X. Feng and K. Mullen, *ACS Nano*, 2013, **7**, 3598-3606.

- 13 M. Alanyalioglu, J. J. Segura, J. Oro-Sole and N. Casan-Pastor, *Carbon*, 2012, **50**, 142-152.
- 14 L. Niu, M. Li, X. Tao, Z. Xie, X. Zhou, A. P. A. Raju, R. J. Young and Z. Zheng, *Nanoscale*, 2013, **5**, 7202-7208.
- 15 M. Zhou, J. Tang, Q. Cheng, G. Xu, P. Cui and L-C. Qin, *Chem. Phys. Lett.*, 2013, **572**, 61-65.
- 16 J. I. Paredes, S. Villar-Rodil, P. Solis-Fernandez, A. Martinez-Alonso and J. M. D. Tascon, *Langmuir*, 2009, **25(10)**, 5957-5968.
- 17 M. K. Punith Kumar, Monika Nidhi and Chandan Srivastava, *RSC Adv.*, 2015, **5**, 24846-24852.
- 18 M. K. Punith Kumar, S. Shanthini and Chandan Srivastava, *RSC Adv.*, 2015, **5**, 53865-53869.
- 19 A. L. Patterson, *Phys. Rev.*, 1939, **56**, 978-982.
- 20 Hongtao Chu, Jinqiu Zhang and Maozhong An, *Int. J. Electrochem. Sci.*, 2013, **8**, 1871-1884.
- 21 M. Sajjadnejad, A. Mozafari, H. Omidvarc and M. Javanbakht, *Appl. Surf. Sci.*, 2014, **300**, 1-7.
- 22 M. K. Punith Kumar and C. Srivastava, *Mater. Charact.*, 2013, **85**, 82-91.
- 23 A. Vlasa, S. Varavara, A. Pop, C. Bulea and L. M. Muresan, *J. Appl. Electrochem.*, 2010, **40**, 1519-1527.
- 24 S. Ranganatha and T. V. Venkatesha, *RSC Adv.*, 2014, **4**, 31230-31238.
- 25 M. Mahdavian and M. M. Attar, *Electrochim. Acta*, 2005, **50**, 4645-4648.

Figures:

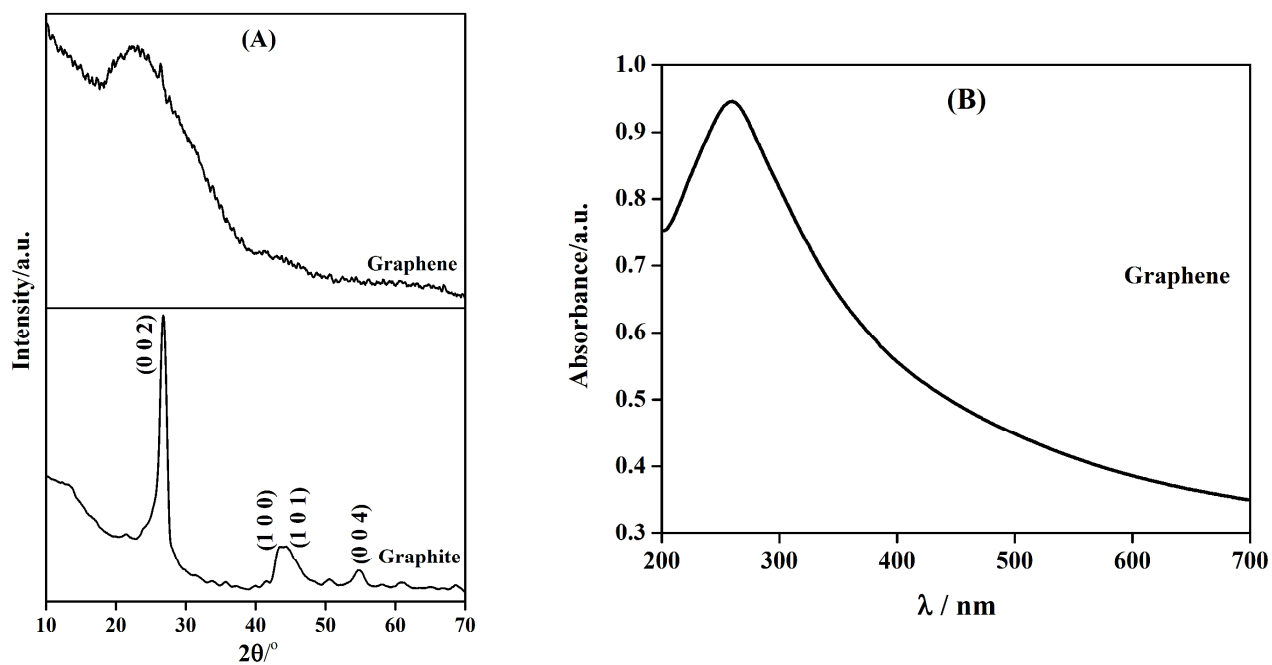


Fig. 1 (A) XRD pattern for graphite (below) and graphene (above) (B) UV-Visible absorption spectrum for exfoliated graphene

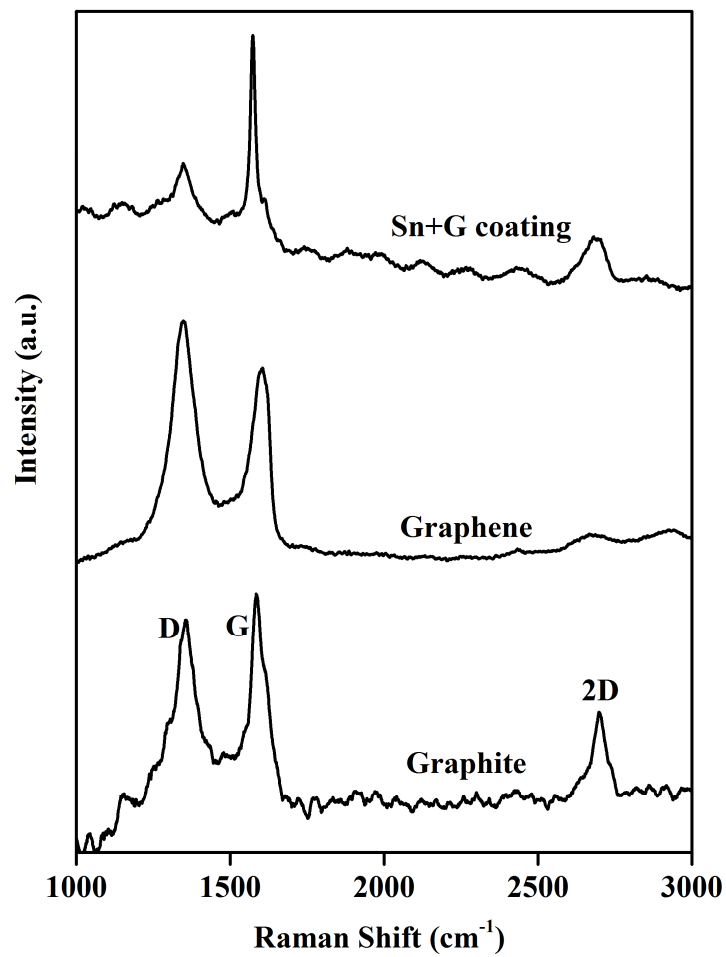


Fig. 2 Raman spectra of graphite, graphene and Sn+G composite coating

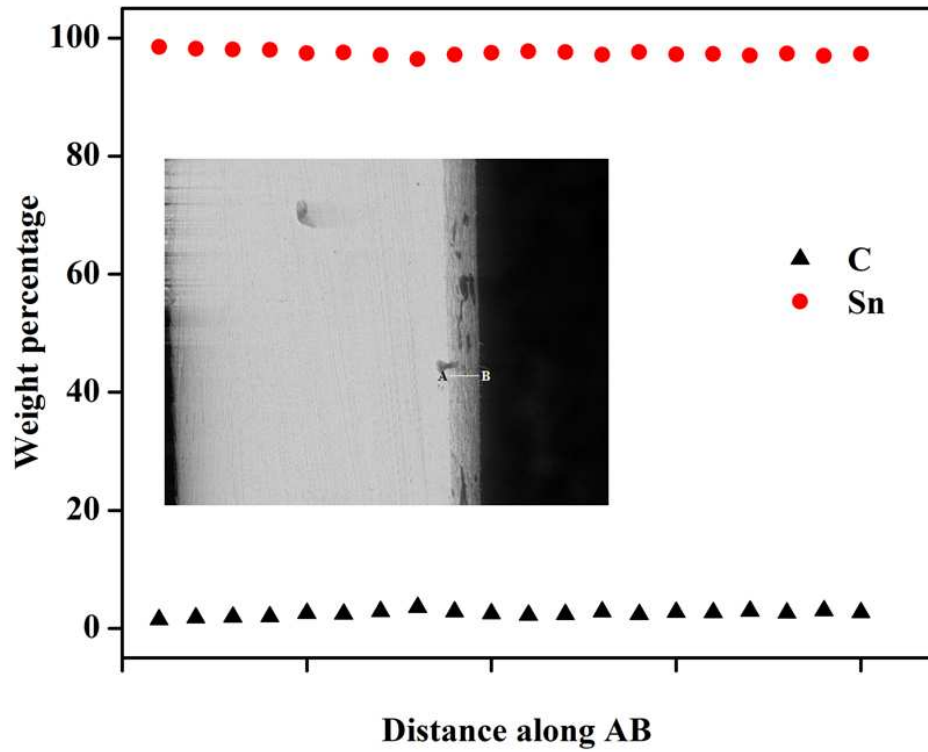


Fig. 3 Compositional line profile obtained from the EDS analysis over the cross section (insert) of Sn+G composite coating.

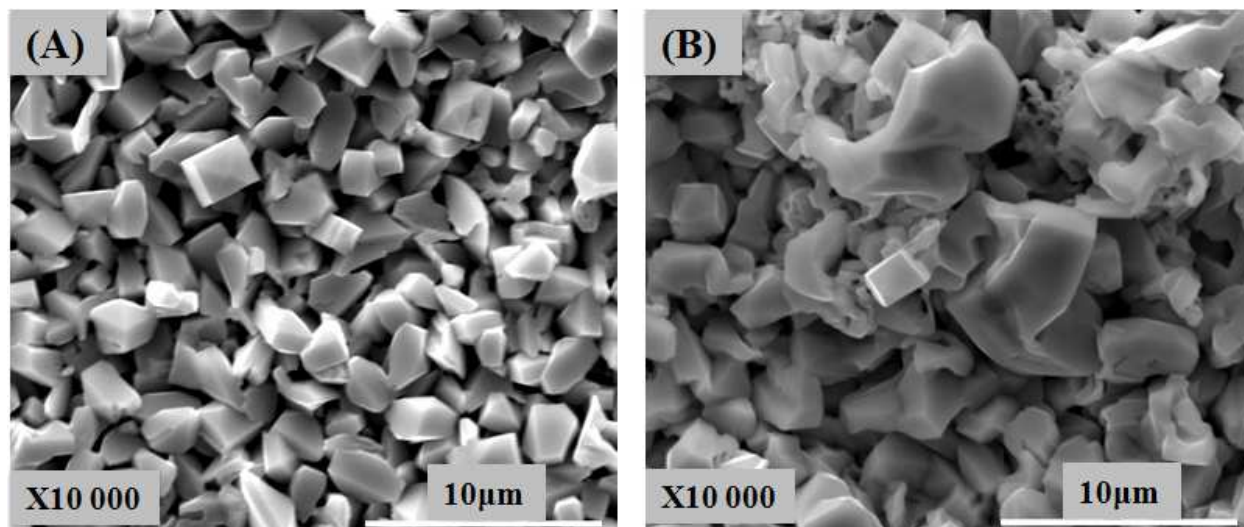


Fig. 4 Representative Scanning Electron Micrographs for (A) Pure Sn coating (B) Sn+G composite coating.

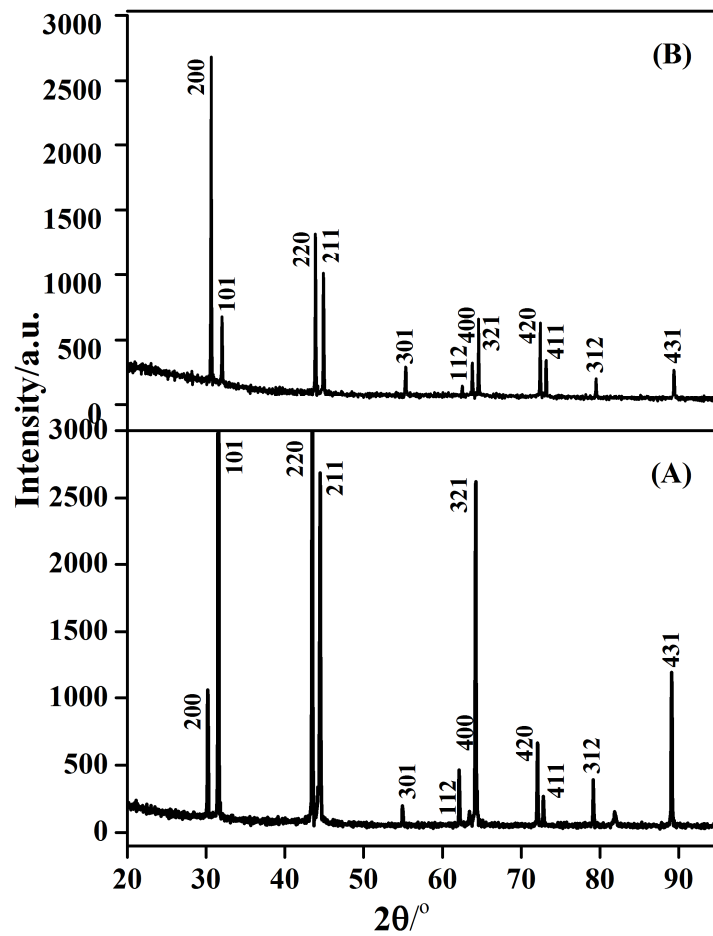


Fig. 5 XRD profile for (A) Pure Sn coating and (B) Sn+G Composite coating

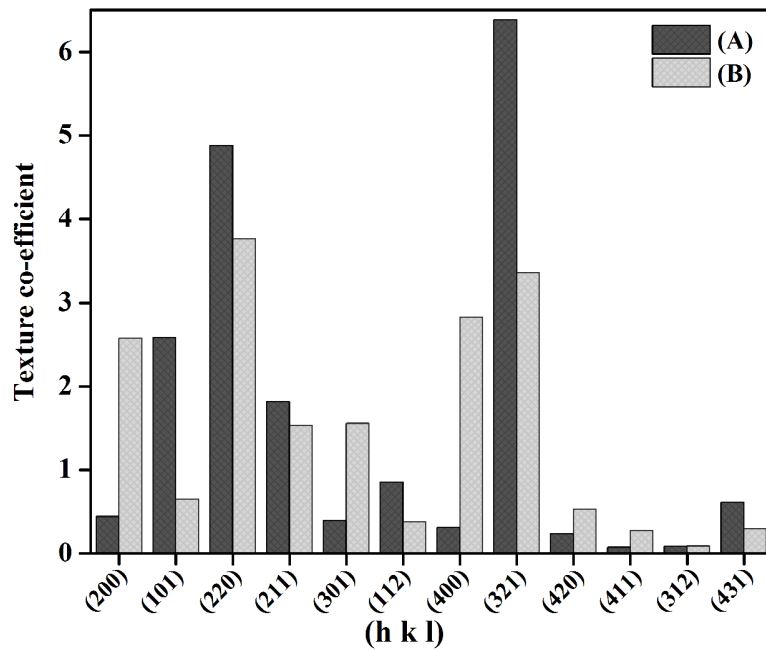


Fig. 6 Texture Orientation of (A) Pure Sn coating and (B) Sn+G Composite coating

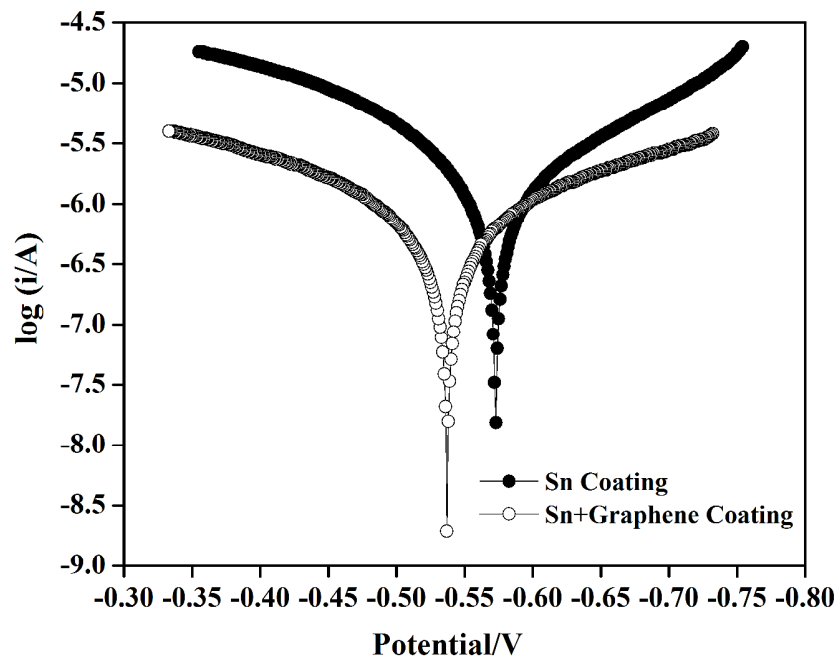


Fig. 7 Tafel Polarization curves for Sn and Sn+G composite coating in 3.5 wt% NaCl electroactive medium.

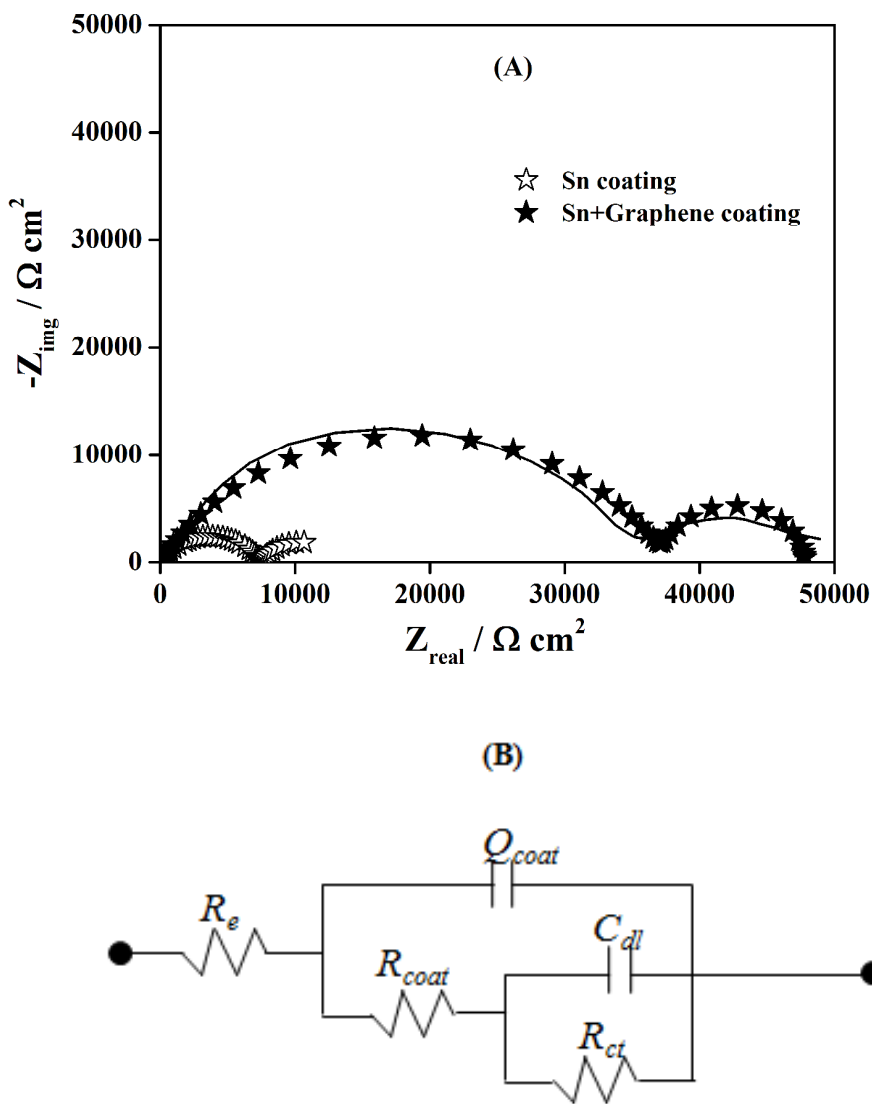


Fig. 8 (A) Impedance Nyquist graph for Pure Sn and Sn+G composite coating (line representing measured data and the symbols representing simulated data) and (B) Electrical equivalent circuit used for simulation of EIS data.

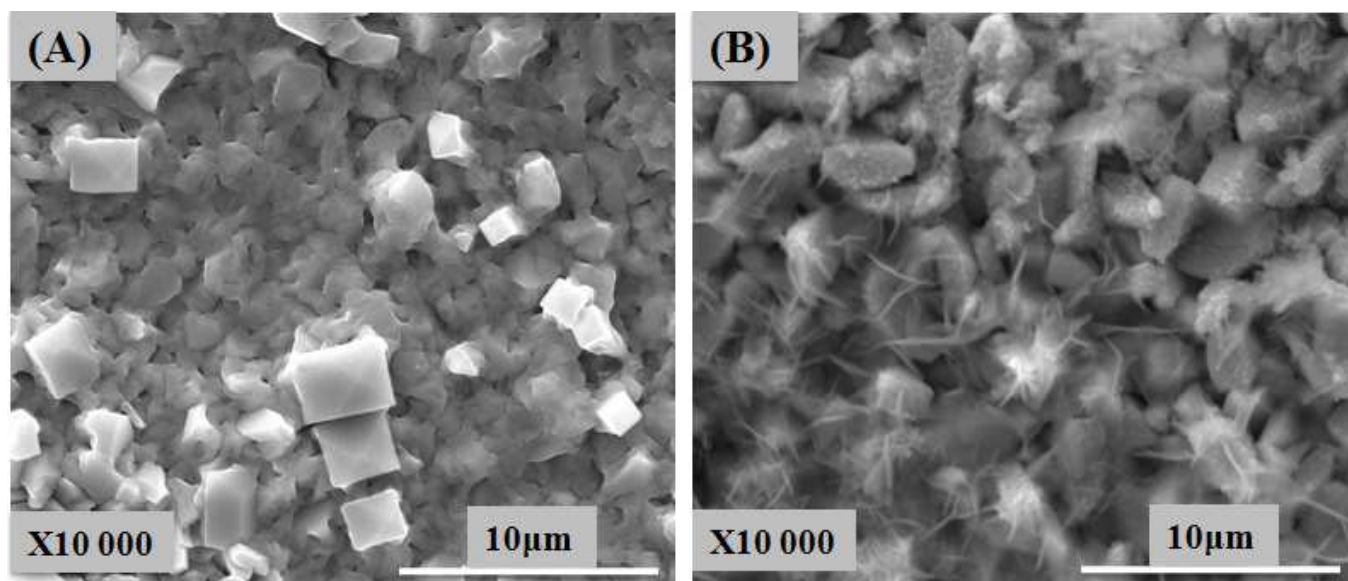


Fig. 9 SEM micrographs of (A) Sn and (B) Sn+G composite coating surfaces after polarization measurement in 3.5% NaCl